

# Electrical generation of stationary light in random scattering media

S. M. Redmond, G. L. Armstrong, H.-Y. Chan, E. Mattson, A. Mock, B. Li, and J. R. Potts

*Department of Electrical Engineering and Computer Science, University of Michigan,  
Ann Arbor, Michigan 48109-2122*

M. Cui

*Department of Physics, Randall Laboratory, University of Michigan, Ann Arbor, Michigan 48109-1120*

S. C. Rand

*Department of Electrical Engineering and Computer Science and Department of Physics, Randall Laboratory,  
University of Michigan, Ann Arbor, Michigan 48109-2122*

S. L. Oliveira

*Instituto de Física de São Carlos, Universidade de São Paulo, São Carlos, CP 369 CEP 13560-970 Brazil*

J. Marchal, T. Hinklin, and R. M. Laine

*Department of Materials Science and Engineering, University of Michigan, Ann Arbor, Michigan 48109-2136*

Received May 23, 2003; revised manuscript received August 27, 2003; accepted August 27, 2003

In recent years there has been great interest in controlling the speed of propagation of electromagnetic waves. In gases and crystals, coherent techniques have been applied to alter the speed of light without changing the physical or chemical structure of the medium. Also, light transmitted by highly disordered solids has exhibited signatures of Anderson localization, indicating the existence of a regime of “stopped” light that is mediated by random elastic scattering. However, to date, light has not been generated in a random medium as a point-like excitation that is fixed in space from the outset. Here we report experimental evidence for the electrical generation and confinement of light within nanosized volumes of a random dielectric scattering medium in which a population inversion has been established, and discuss the properties of these novel light sources.

© 2004 Optical Society of America

OCIS codes: 290.0290, 290.4210, 030.0030.

## 1. INTRODUCTION

Recently, coherent optical techniques have been applied in the laboratory to reduce the velocity of light in selected media, making it nearly stationary. In early experiments<sup>1–4</sup> light was converted into a nonradiative excitation of the medium to achieve this result—creating “dark” states or “dark” polaritons—while a recent proposal<sup>5</sup> and experiment<sup>6</sup> discuss speed reduction of a propagating wave that maintains some of its “bright,” radiative character. However, in the present paper we introduce a different concept for producing zero-velocity light—one that is not based on the interaction of coherent waves—that shows it is not necessary to begin with propagating waves and slow them down by utilizing ultrahigh dispersion or other means. Instead, light can be created as a bright field excitation that, from the outset, does not have the form of a propagating wave at all. In this paper, experimental results are presented for what we believe to be the first experimental realization and characterization of stationary light sources of this kind.

Our approach is to generate light emission in media in

which negligible absorption exists and in which ordinary light propagation is prevented by elastic scattering. The idea is to produce stimulated emission that, as a result of the scattering, is neither absorbed nor allowed to propagate away from the near-field region of the source, a situation reminiscent of propagation in media with purely imaginary indices of refraction in which propagation is forbidden. It is helpful to begin by considering evanescent fields in a familiar context before turning to experimental evidence and a discussion of nonpropagating forms of light in multiple-scattering systems.

Low-frequency electromagnetic waves are reflected from plasmas whenever the medium acquires a negative (relative) permittivity  $\epsilon_r$ . Transmission of radio waves is prevented and the incident wave is totally reflected without any loss of energy if the frequency is below a critical value. It is well established that at night total external reflection of this type from the ionosphere often occurs at short-wave frequencies, much to the delight of amateur radio enthusiasts whose communication range is thereby extended.<sup>7</sup> Thus, for waves impinging on the ionosphere

from the lower atmosphere, total external reflection of the field from the plasma layer is commonplace. It is not common, however, to analyze low-frequency waves generated deep within a plasma that experience total internal reflection in three dimensions.

Electromagnetic waves at frequencies below the plasma frequency  $\omega_p$ , far from any absorptive resonances, develop a purely imaginary refractive index  $n = \sqrt{-|\epsilon_r|} = in'$ , where  $n'$  is a positive real number. Any electromagnetic field of the form  $E(R, t) = (E_0/R)\exp[i(n\bar{k}_0\bar{R} - \omega t)]$ , where  $R$  is the distance from the origin (inside the medium), then decays exponentially in space:  $E(R, t) = (E_0/R)\exp(-n'\bar{k}_0\bar{R} - i\omega t)$ . If the wave can neither be absorbed nor reach the radiation zone readily, it must be totally reflected inside a volume of the medium on the order of a cubic wavelength in size, exhibiting rapid attenuation in all directions, harmonic variation in time, but no periodic oscillations in space. Assuming that the emission process takes place irreversibly, the spatial envelope of the resulting electromagnetic disturbance will be time-independent. Such a process illustrates a potential means whereby electromagnetic radiation could be generated in a quasi-stationary state: a state that is nonpropagating and has an envelope that changes very little on time scales far greater than the temporal oscillation period.

This example applies to electromagnetic sources within structureless media containing free charges, but in the remainder of this paper we shall be concerned with the adaptation of this concept to atomic emission within dielectrics, in which there are no free charges. We address the interesting question whether light can be stationary in isolated portions of random, transparent dielectrics without consuming or converting the electromagnetic energy into some other form.

There exists a considerable body of literature on localization of light in photonic bandgap materials<sup>8</sup> and in random media.<sup>9</sup> Light can be localized in wavelength-sized regions by surrounding a small volume with lossless Bragg structures that prevent light from propagating outward by simply reflecting it back to the origin. This approach to electromagnetic confinement relies on carefully engineered, regular structures with zero density of states, whereas our results involve all modes of space. Similarly, the phenomenon of Anderson localization<sup>10–13</sup> is known to diminish wave mobility when a sufficient degree of disorder in a system is reached. To halt electromagnetic transport through disordered media, many researchers have concentrated on maximizing the “stopping power” of individual scattering events to localize electromagnetic waves,<sup>14–16</sup> a strategy that works especially well under controlled conditions near Mie scattering resonances<sup>17</sup> by using particles close to a wavelength in size to maximize the effect of independent scattering. This, too, differs from the approach developed in this paper, which relies instead on “dependent” rather than “independent” multiple scattering among dense subwavelength particles in an active, disordered medium. Dependent scattering includes fully coherent field addition. In this paper we present results consistent with the conclusion that novel interference effects in multiple scattering from dense collections of particles smaller than a

wavelength in diameter can make up for low index contrast and small scattering cross sections that would otherwise prevent localization by dielectric nanoparticles.

## 2. THEORETICAL BACKGROUND

In several published experiments on stopped light, external light fields have been applied to cause absorptive media to become transmissive through the phenomenon of electromagnetically induced transparency.<sup>18</sup> To trap or “store” light energy in a state of polarization of the medium that neither propagates nor radiates (a dark polariton), the coupling or control field is momentarily switched off in these experiments. Light is thereby stored as a nonradiative excitation of the medium that can be converted back into propagating light by restoring the coupling field after a short delay. This method of light storage by conversion into a two-photon coherence has been demonstrated in gases and solids.<sup>1–4</sup> Here we present evidence that suggests light can also be stored in lossless, random dielectrics without such conversion, in the form of a bright polariton.

A well-known relation in optics provides a clue to new possibilities for generating electromagnetic radiation that is losslessly localized in space. The generalized optical theorem,<sup>19</sup> exactly applicable in three dimensions, provides the necessary insight into the balance between wave energy densities, gains, and losses in nonuniform—even random—media. For our purposes it is sufficient to consider its one-dimensional form for plane waves.<sup>20</sup> We consider the incident, reflected, and transmitted intensities  $|E_i|^2$ ,  $|E_r|^2$ , and  $|E_t|^2$ , respectively, of an electromagnetic wave impinging on a lossless, dielectric medium of thickness  $l$ , and relate them to the intensity  $|E|^2$  inside the slab where the relative permittivity is  $\epsilon_r(z)$ :

$$|E_i|^2 = |E_t|^2 + |E_r|^2 + k_0 \int_{-l/2}^{l/2} |E|^2 \text{Im}[\epsilon_r(z)] dz. \quad (1)$$

Here  $k_0$  is the vacuum wave number given by  $k_0 = \omega/c$ .

Note that because  $\epsilon_r$  may vary with position  $z$ , the properties of the dielectric slab can fluctuate. Ordinarily, we associate the integral in Eq. (1) with absorptive losses [ $\text{Im}(\epsilon_r(z)) \neq 0$ ] that cause dissipation rather than the storage of energy. However, by creating a population inversion we convert loss to gain. In inverted media we encounter both the imaginary component of susceptibility and the nonzero internal field necessary to make a contribution to Eq. (1) that is opposite in sign to an absorptive loss. By introducing near-field multiple scattering through nanostructure of the medium, as we show below, the internal field can also be greatly enhanced in microscopic regions of the sample. The energy density in Eq. (1) thereby becomes nonzero and nonuniform. Because Eq. (1) is implicitly a steady-state relation, this reflects not just an increased flow of energy, but indicates the presence of light that resides in small regions of the dielectric. Hence, in strongly scattering, “active” dielectrics, the energy density of an incident wave can be separated into transmitted, reflected and stored portions. Energy is derived from the source of gain and stored where the field  $E$  is largest. Where the field energy is

confined to regions smaller than a wavelength in size, the stored light can be designated stationary light to distinguish it from propagating modes of all kinds. Since we must have both  $E \neq 0$  and  $\text{Im}[\epsilon_r(z)] \neq 0$  to store light in this way, this method is based on bright field polarization, unlike the dark polariton approach that is characterized by an average field of zero magnitude.

For the energy densities associated with stationary light regions to be significant in active, random scattering media, the gain and internal field must be maximized together according to Eq. (1). There are numerous approaches to optimizing gain in homogeneous media,<sup>21</sup> but methods to enhance internal fields in strong scatterers have received little attention. This is not surprising, because large enhancements are the result of overlapping fields from dependent (to be distinguished from independent) scattering events<sup>22</sup> among closely packed, subwavelength particles.<sup>23</sup> Lossless, dependent scattering media are difficult to synthesize and exact analysis of their electromagnetic properties is an unsolved problem in three dimensions. Previous efforts to halt the transport of light through the use of elastic scattering have avoided the dependent scattering regime for precisely this reason.

In Fig. 1(a) the results are given of a one-dimensional (1D) numerical calculation of the internal field  $E$  of a random dielectric that takes dependent scattering into ac-

count exactly and explores its effectiveness for local field enhancement. Interlayer interference effects can cause field fluctuations in dielectric systems that are large and distinct in origin from other local field phenomena, such as plasmon resonances in metals.<sup>24</sup> We applied a transfer-matrix method<sup>25</sup> to a randomly sampled, log normal distribution of 80-nm “particles” (dielectric layers) with a FWHM of 60 nm. Spacings between layers were taken to be Gaussian distributed with a mean spacing of 15 nm and a FWHM of 3 nm at  $\lambda = 405$  nm. The first distribution was chosen to reflect the particle sizes typical of the pyrolysis technique used to synthesize our nanopowders. The second corresponds roughly to experimental densities.

As evidenced by Fig. 1(a) large field enhancements are theoretically possible in random, one-dimensional scattering systems, yielding peak ratios of  $E$  to the total input field  $E_0$  of over  $10^2$  within regions a mere wavelength in extent. Despite severe variations in the assumed particle positions and sizes, energy density enhancements of over  $10^4$  are therefore predicted in subwavelength (1D) domains. Dependent scattering can clearly exert an important influence over propagation, enabling light storage (and localization) in some lossless dielectrics, at least at low dimensionality.

We also examined the electric field of a dipole radiating

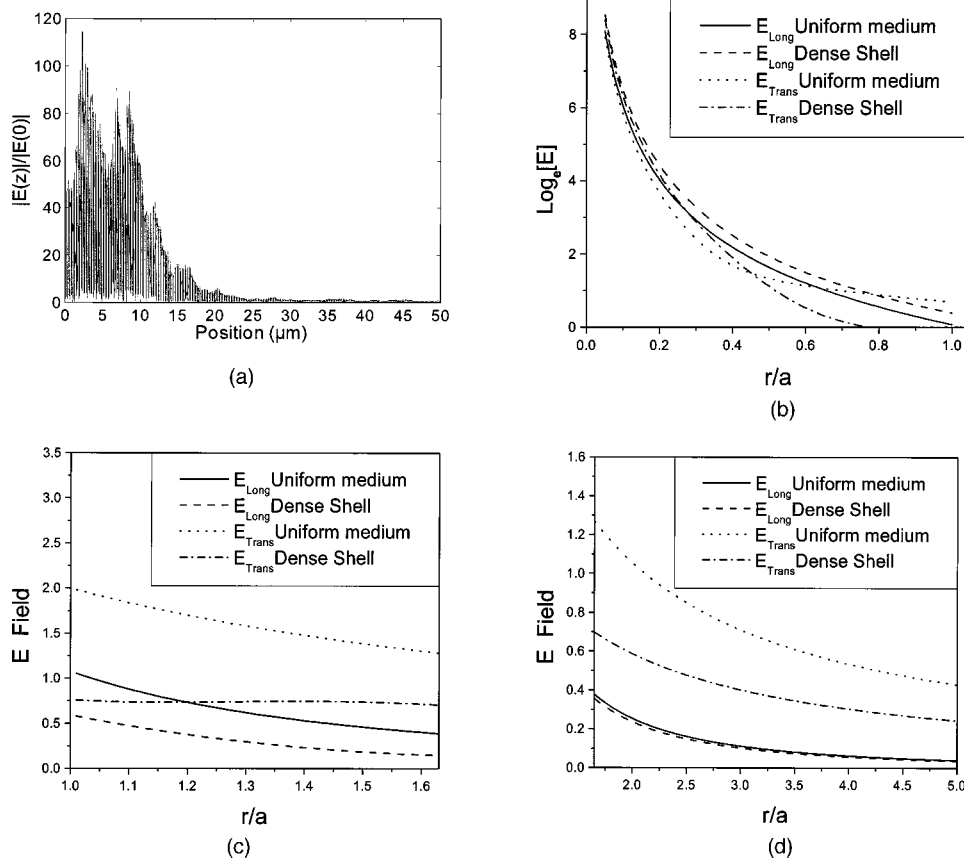


Fig. 1. (a) Magnitude of the internal electric field (exact 1D model with dependent scattering to all orders). Results shown are for a single (random) configuration of lossless dielectric nanoparticles ( $\epsilon_r = 3.06$ ) with mean diameter  $\phi = 80 \pm 30$  nm and mean spacing  $15 \pm 3$  nm at  $\lambda = 405$  nm. (b), (c), (d) Plots of the longitudinal and transverse fields emitted by a dipole at the origin of three uniform, spherical regions compared with corresponding values for a uniform, featureless solid. In regions 1 ( $r < a$ ), 2 ( $a < r < b$ ), and 3 ( $r > b$ ), assumed values were  $\epsilon_1 = 1$ ,  $\epsilon_2 = 2.5$ , and  $\epsilon_3 = 1$ , respectively, and for the uniform medium  $\epsilon = 2.5$ . The sizes of regions 1 and 2 were  $a = \lambda_1/4$  and  $b = (\lambda_1 + \lambda_2)/4$ , where  $\lambda_i = \lambda_0/(\epsilon_i)^{1/2}$  is the wavelength in region  $i$ .

within a three-dimensional (3D) dielectric medium where inhomogeneities exist, but where dependent scattering is ignored. This was done to see if density fluctuations contribute independently to field enhancement. By using Mie theory<sup>26</sup> the electric field magnitude was calculated in all regions of space for a three-shell model. Region 1 with a dipole at its center was surrounded by a thin spherical shell (region 2) and an embedding medium (region 3). When permittivities of  $\epsilon_1 = 1$  and  $\epsilon_2 = \epsilon_3 = 2.5$  were assigned to the corresponding regions, it was found that the Hertz vector  $\Pi_z$  within pores of radius  $a \ll \lambda$  could easily exceed that for uniform media by factors of 100 or more. However, despite its proportionality to  $\Pi_z$  (as well as to the gradient of  $\text{div } \Pi_z$ ), the electric field was everywhere less than twice that of a uniform solid ( $\epsilon_1 = \epsilon_2 = \epsilon_3 = 2.50$ ). Although this enhancement was small, it exceeded the ratio of local field factors  $|E_{\text{sol}}/E_{\text{vac}}| = (\epsilon_{\text{sol}} + 2)/(\epsilon_{\text{vac}} + 2) = 1.5$  at certain radii, and showed large variations within regions of constant permittivity. For example, with effective permittivities of  $\epsilon_1 = 1$ ,  $\epsilon_2 = 2.5$ , and  $\epsilon_3 = 1$ , corresponding to a dense shell in region 2, transverse field values within the pore and the shell revealed ratios varying between 0.4 and 1.7 compared with a uniform medium. This is illustrated in Figs. 1(b), (c), and (d) for  $k_1 a = \pi/2$  and  $k_2(b - a) = \pi/2$ . Similar results were obtained for calculations with other values of  $a$ ,  $b$ , and  $\epsilon$ .

Near the origin both the longitudinal and transverse field magnitudes exceeded those in a uniform medium. In the dense shell (region 2) the transverse component in Fig. 1(c) actually grew, rather than decreasing in the usual manner. Additionally, in the far field ( $r > b$ ) both components were suppressed compared with the uniform medium. Since constant local field factors should yield constant separation of curves on a logarithmic plot such as Fig. 1(b), other factors are needed to account for the crossings in this figure. This reveals nontrivial field enhancements that depend on density fluctuations, although no evidence of morphological resonances was found with this shell model.

These results show that dependent scattering and sub-wavelength fluctuations in density can independently contribute to field enhancement in random nanomedia. They provide a partial understanding of possible origins of field enhancements inferred from experiments on random dielectric nanomedia reported below. However, these initial results ignore the possibility that density fluctuations and dependent scattering may act together in the strong scattering regime to produce large 3D enhancements of local fields. Numerically exact results capable of accurately accounting for dependent scattering in the presence of density fluctuations are needed to explore the question of field enhancements in dense 3D random media more fully.

In the remainder of this paper, evidence for enhanced internal fields is sought experimentally from several different kinds of observations in dense nanopowder samples. In Section 3 laser transmission and speckle correlation measurements through free-standing powders are analyzed. It is found that, while multiple scattering causes a real enhancement in absorption, neither the degree of enhancement nor the very long characteristic

length scales for transmission are well explained by the diffusion theory of optical transport in our dense, nanoparticle samples. At the same time, the measurement of coherence length with spatial correlation techniques provides evidence of field randomization on very short length scales (on the order of a wavelength) in agreement with earlier coherent backscattering results. Hence, two very different length scales emerge from these observations. It seems perplexing that directional randomization of a wave can occur over distances as short as a wavelength and yet significant amounts of energy propagate a millimeter or more. In Section 4 we offer a resolution of this apparent discrepancy which sheds light on observations of cw laser emission from optical feedback regions with dimensions smaller than a wavelength. We conclude with direct evidence of light field enhancement in a random medium and stationary light generation.

### 3. SCATTERING CHARACTERISTICS OF DENSE, RARE-EARTH-DOPED NANOPOWDERS

Our experiments made use of  $\text{Y}_2\text{O}_3$  and  $\text{Al}_2\text{O}_3$  nanopowders with particle sizes and filling fractions corresponding to more than one hundred scattering particles per wavelength. A reduction in the single-particle scattering cross section (incurred by the use of subwavelength particles) was accepted in order to allow near-field, coherent overlap effects to take place. Strong dependent scattering effects arise only when many scattering events take place within a distance short compared to the spatial period of the wave. This requires that near fields from adjacent scatterers overlap,<sup>22</sup> a condition that enormously complicates theoretical analysis, but in view of the results of Fig. 1 mediates the appearance of interesting, confined-field regions.

Paradoxically, as shown below, for subwavelength separations of particles that are themselves less than a wavelength in size, an increasing amount of light energy is found to flow right through the medium as the scattering mean free path falls below half a wavelength. As porosity goes to zero, one rapidly approaches the limit of fully dense, nonabsorbing solids through which incident light is, of course, easily transmitted. (Note that a similar effect accompanies porosities that approach one. Transmission also rises as the solid volume fraction drops because there is very little matter to scatter the light. The scattering mean free path within particle clusters can remain subwavelength in scale, but the sample is mostly empty space and free propagation takes place outside the clusters).

Transmission data were obtained for samples of 1% Yb: $\text{Y}_2\text{O}_3$  with an average particle size of 30 nm. Free-standing powder layers were prepared in the form of disk-shaped wedges by applying a pressure of 2 lb/in.<sup>2</sup> The 3° wedges had a minimum thickness of 150  $\mu\text{m}$  and a diameter of 2.0 cm. Angle-integrated, forward transmission was then measured versus sample thickness  $l$  and fitted using Eq. (10) of Ref. 27. The transmission is well approximated by  $T(l) \approx \exp(-l/\xi)$  for sample thicknesses exceeding the absorption length,<sup>28</sup> so it is readily seen from the inset of Fig. 2(a) that experimental attenuation

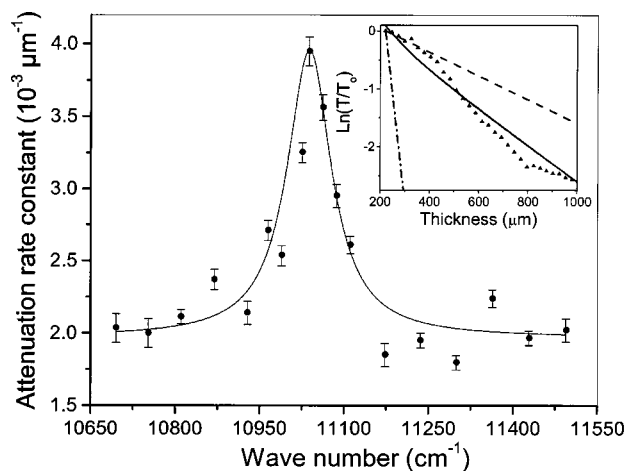
length scales  $\xi$  exceed the transport path length  $l^*$  by three orders of magnitude. It seems perplexing that real samples which directionally scramble light within half a wavelength ( $l^* < \lambda/2$ ), as we previously reported,<sup>29</sup> still transmit light over macroscopic distances [see Fig. 2(a) where  $T \sim 0.1\%$  for  $l \sim 1000 \mu\text{m}$ ]. However, this is not inconsistent with an exact simulation of dense 1D samples based on the transfer-matrix method. In Fig. 2(b) results are given for simulated transmission through nanopowders similar to the samples in this work. The calculation sampled a log normal distribution of particle sizes typical of pyrolytic synthesis by selecting a mean diameter of 155 nm (with FWHM = 45 nm) to create a random string of dielectric “particles.” The decay of sample transmission with thickness was then calculated for each assumed value of scattering mean-free-path  $l_s$  to derive attenuation distances  $\xi$  at  $\lambda = 906 \text{ nm}$  for a medium with the relative permittivity of yttria ( $\epsilon = 3.24$ ). Semilogarithmic decay lengths for 25–50 complete configurations of up to 10,000 particles were averaged for each mean particle spacing ( $l_s$ ) in the range 25 nm–100  $\mu\text{m}$  by use of a randomly-sampled Gaussian distribution of fixed percentage half-width (FWHM = 12%). The average values of  $\xi$  decreased linearly with  $l_s$  until the high density limit ( $l_s \leq \lambda$ ) was reached, whereupon surprisingly large Mie-like resonances and long attenuation lengths appeared despite the lack of regularity in particle position and size.

Short mean free paths and subwavelength transport distances seem incongruous in the face of long attenuation lengths. Yet this combination is an important feature of optical transport in ultrafine random media consisting of nanoparticles causing dependent scattering as shown below. Experimental evidence of the failure of diffusion theory that was obtained from simple absorption measurements through our samples is considered next.

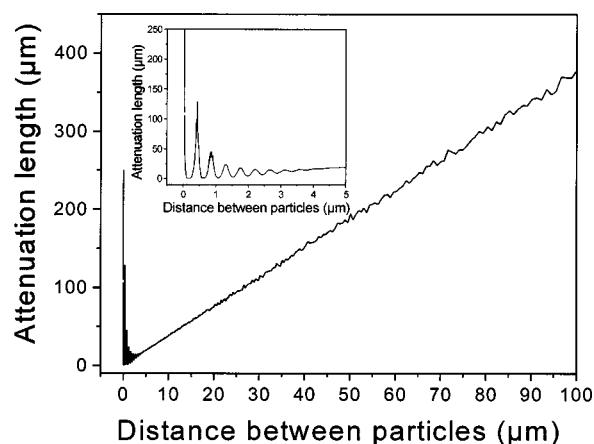
In Fig. 2(a) the measured attenuation-rate coefficient of light transmitted through thin powder layers at wave-

lengths near the  $\text{Yb}^{3+} [{}^2F_{7/2}(0) \rightarrow {}^2F_{5/2}(2')]$  resonance at 906 nm is found to be an order of magnitude greater than expected. By using the off-resonance value (at 870 nm) for the semilogarithmic slope of transmission  $\xi^{-1} = 1.96 \times 10^{-3} \mu\text{m}^{-1}$ , together with the peak extinction length on resonance, namely  $l_{\text{res}}^{-1} = 3.08 \times 10^{-3} \mu\text{m}^{-1}$  from Fig. 2(a), we estimate the experimental Yb-related absorption length by using the simple relation<sup>30</sup>  $l_{\alpha}^{-1} = l_{\text{res}}^{-1} - \xi^{-1} = 1.12 \times 10^{-3} \mu\text{m}^{-1}$  to be  $l_{\alpha} = 893 \mu\text{m}$ . This value is a factor of 8 shorter than the absorption length  $l'_{\alpha} = 7.0 \text{ mm}$  calculated for isolated Yb ions of the same density  $N = 4.1 \times 10^{20} \text{ cm}^{-3}$  (based on the established cross section in this host,  $\sigma_{\text{abs}} = 0.35 \times 10^{-20} \text{ cm}^2$ ,<sup>31</sup> and the measured filling fraction 0.15). This shows directly that there is a very large enhancement of absorption due to multiple scattering.

To determine whether the enhanced absorption within our samples was principally the result of long diffusion paths or dependent scattering within enhanced field regions, we made spatial correlation measurements and a quantitative comparison with diffusion theory. Figure 3 gives the spatial intensity–intensity autocorrelation of a He–Ne laser speckle pattern that was transmitted through a free-standing sample of 30-nm particles and recorded with a CCD camera (Princeton Instruments EEV 576  $\times$  384) at  $\lambda = 632.8 \text{ nm}$ . Individual pixels had dimensions of  $22 \times 22 \mu\text{m}^2$  and dark counts of 6–8 electrons/s. Frame times were 17 ms. The sample exit surface and the active area of the camera were located in the front and back focal planes of the transform lens, respectively (N.A. = 1). A relay telescope was used to adjust the illumination spot diameter to 0.48 (solid curve) and 0.68 (dashed curve) of the side length of the active readout area ( $384 \times 384$  pixels). This permitted us to demonstrate that the minor ripple structure at the base of the correlation peak arose entirely from finite aperture effects in the image (transform) plane, and not from the



(a)



(b)

Fig. 2. (a) Measured transmission through free-standing  $\text{Yb}^{3+}:\text{Y}_2\text{O}_3$  nanopowder wedges. The inset shows raw data (triangles) versus thickness at 906 nm. The dashed curve gives the (calculated) single-pass absorption for the experimental Yb concentration of  $N = 4.1 \times 10^{20} \text{ ions/cm}^3$  at volume fraction 0.15 plus the experimental off-resonance scattering attenuation. The dotted–dashed curve is the result of diffusion theory (see text). (b) Calculations of attenuation length versus mean free path through lossless dielectric particles ( $\epsilon = 3.24$ ) of mean diameter 155 nm at  $\lambda = 907 \text{ nm}$ . The inset magnifies the high-density region where Mie-like resonances are evident and the attenuation length diverges as the mean free path approaches zero.

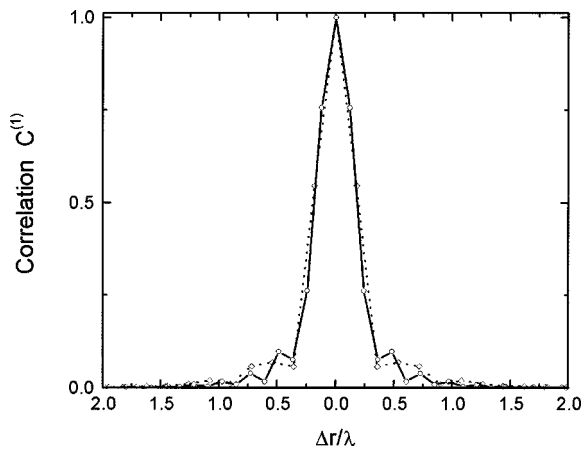


Fig. 3. Spatial autocorrelations of laser speckle recorded at  $\lambda = 632.8$  nm in transmission through yttria nanopowder (at 0.15 filling fraction). The solid and dashed curves correspond to different spot diameters at the camera (0.48 and 0.68 times the length of the active area, respectively).

intensity–intensity correlation itself. The displacement axis in Fig. 3 was calibrated by recording the far-field diffraction pattern of Ronchi rulings spaced by  $50 \mu\text{m}$  and inverting the image as described next.

To convert the far-field speckle pattern to a near-field correlation plot, data from the CCD were squared and inverse-Fourier-transformed to furnish the intensity–intensity correlation function  $C^{(1)}$  at the sample surface. The oscillatory nature of this function,<sup>32</sup> given by  $C^{(1)} = \exp(-\Delta r/l_s \text{sinc}^2 k\Delta r)$ , has been observed previously in the optical domain.<sup>33</sup> Because the experimental correlation traces presented in Fig. 3 show no evidence of the  $\text{sinc}^2 k\Delta r$  factor in  $C^{(1)}$ , which has a period of  $\lambda/2$  but only small variations that depend on the inverse diameter of the spot illuminating the CCD and the wavelength, the exponential envelope of  $C^{(1)}$  evidently decays with a characteristic length less than  $\lambda/2$ . This permits an upper limit of  $l_{\text{coh}} = l_s < \lambda/2 = 316$  nm to be set on the longitudinal coherence distance of the sample, thus confirming that dephasing takes place on the same subwavelength distance scale with respect to forward propagation as directional randomization in the backward direction ( $l^* \sim 311$  nm<sup>29</sup>). By taking the mean free transport distances in the forward and backward directions to be equal ( $l_f^* = l_b^*$ ) on this basis, an absorption length of  $l_\alpha^D = (l_\alpha l^*/3)^{1/2} = 27 \mu\text{m}$  is predicted by diffusion theory.<sup>28,34</sup> This value of  $l_\alpha^D$  is much shorter than the experimental absorption length  $l_\alpha = 893 \mu\text{m}$  determined above, and we conclude that diffusion theory underestimates the absorption length by more than an order of magnitude.

This failure of diffusion theory is not all that surprising. Goodman pointed out long ago that a coherence length less than an optical period ( $l_{\text{coh}} < \lambda$ ), as the analysis here indicates is the case, corresponds to an evanescent or nonpropagating wave.<sup>35</sup> Since diffusion theory does not include contributions from nonpropagating field components, it cannot be expected to account fully for the energy density in dense random media where dependent scattering may give rise to stationary light. Our speckle measurements support the idea that significant contribu-

tions to absorption come from small, dependent-scattering regions that are not well described by diffusion theory. In Section 4 we provide additional evidence of field confinement and stationary light within our samples in experiments on cw random lasing processes.

#### 4. CONTINUOUS-WAVE RANDOM LASER EXPERIMENTS

There have been many previous reports of laser action in random gain media.<sup>36–40</sup> In all the earlier experiments, however, pulsed optical pumping was used and light was amplified through propagation over trajectories that were many wavelengths in length. In recent work<sup>39,40</sup> macroscopic ringlike trajectories were considered to compose the cavities in which laser action took place, and standard features of coherent lasers such as directionality and frequency selectivity in the output were observed. The separation of modes in individual cavities was consistent with the usual inverse proportionality to round-trip cavity length.<sup>38,40</sup> If overdamped (nonpropagating) waves with a spatial extent of a wavelength or less were generated in a lossless dielectric, however, it is easily understood that no transport of energy around a macroscopic cavity could take place. As a result, stimulated emission from a source of stationary laser light would have characteristics very different from that of conventional lasers or random lasers with coherent feedback. If waves do not propagate far enough for constructive interference from overlapping fields to arise, no frequency (mode) selectivity can appear in stimulated emission from such pointlike random lasers.

In earlier accounts of cw random laser action<sup>29,41</sup> the absence of angular and spectral selectivity was noted, together with sharp threshold behavior and linear output. An electron beam was used in ultrahigh vacuum to pump Nd-doped alumina powder with an average particle size estimated to be 27 nm under conditions in which the transport mean free path  $l^*$  was measured to be less than  $\lambda/2$ . Incoherent laser action was observed at 405 nm above a sharp pumping threshold (Fig. 4). As shown in this figure, the fluorescence lifetime of the emitting level drops when the current exceeds threshold, revealing that the emission rate increases as a result of the onset of stimulated emission as expected. Lifetime measurements required 10 hours of acquisition per point because of low count rates in the presence of electron beam blanking. Because of the lengthiness of this experiment, corresponding measurements of luminescent output (Fig. 4, dashed curve) were made very rapidly, and then only to locate threshold and illustrate the linear output above it. The slight drop in output at a current above  $8 \mu\text{A}$  in Fig. 4 is an experimental artifact. A more representative output curve that shows reproducible linearity and consistent output saturation under the same conditions can be found in Ref. 41.

The maximum gain–length product estimated for a wave propagating one mean free transport length through this particular sample, with an impurity density of  $N(\text{Nd}^{3+}) = 2.5 \times 10^{19} \text{cm}^{-3}$  and emission cross section  $\sigma < 10^{-18} \text{cm}^2$ , is very small ( $\gamma l^* = N\sigma l^* < 10^{-3}$ ). Under these conditions, single-pass amplification yields an

output intensity of only  $I(l^*)/I(0) = \exp(\gamma l^*) \cong (1 + N\sigma l^* + \dots) \sim 1.001$ . So while output power in a low-gain amplifier with these characteristics would be linear in the excited state density  $N$ , amplification would not even be noticeable without cavity feedback. To account for cw laser operation with a sharp change in emission slope at threshold, a very large cavity enhancement factor is necessary. Linearity of the output<sup>41</sup> rules out the pos-

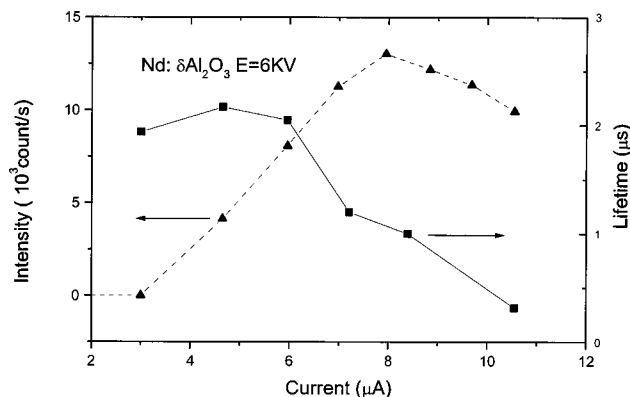


Fig. 4. Measured fluorescence lifetimes (solid curve) and emission intensity (dashed curve) versus current from  $\text{Nd}^{3+}:\delta\text{-Al}_2\text{O}_3$  in the neighborhood of the intensity threshold. Filling fraction and particle size were 0.15 and  $\phi \sim 30$  nm, respectively.

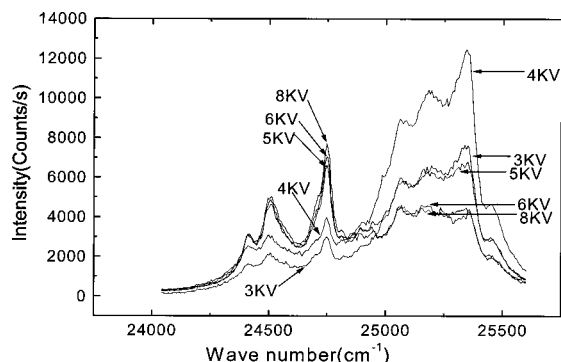


Fig. 5. Spectral emission intensity recorded by cathodoluminescence from  $\text{Nd}^{3+}:\delta\text{-Al}_2\text{O}_3$  nanopowder at various voltages with the total excitation power held constant.

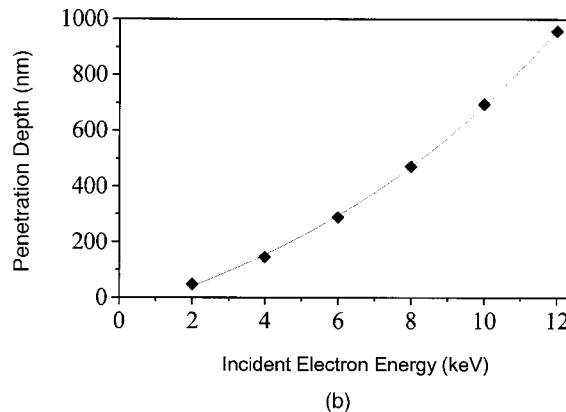
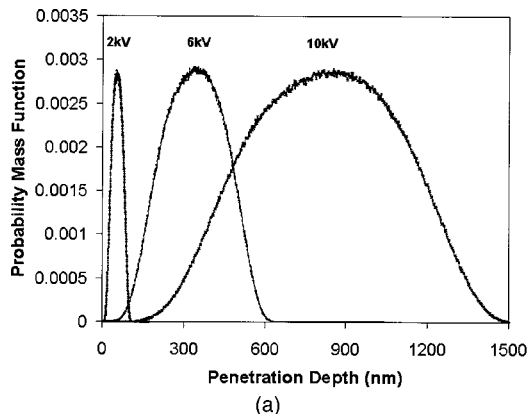


Fig. 6. Monte Carlo simulation of electron penetration versus voltage. (a) Distributions of electron locations after elastic scattering brings them to rest (defined as  $E < 50$  eV) in alumina of 50% solid density. Note the broadening with voltage, which leads to significant dilution of the average excitation density as voltage increases. (b) Mean electron penetration depth versus voltage from the simulations in (a).

sibility that stimulated emission from our samples is merely the result of amplified spontaneous emission. Hence, the subwavelength transport distance, together with large cavity enhancement and lack of speckle, furnish important evidence that cw laser output in our samples is the result of optical confinement in regions less than a cubic wavelength in size. While this in itself is evidence of stationary (laser) light generation within the medium, we sought additional, more direct evidence of electromagnetic confinement, as described next.

There has been no prior investigation of the optical output of a cw random laser purely as a function of electron penetration into the scattering medium.<sup>29,41</sup> It is useful to test the interpretation of our results to date by searching for increased stimulated emission output as the gain volume is moved deeper into the medium. Output should improve if optical confinement by scattering improves away from radiatively lossy surfaces. Such a trend is opposite that expected for radiation originating from near-field components of a classical dipole embedded in a medium near an interface.<sup>42</sup> To measure laser output versus penetration depth experimentally, the energy of incident electrons was therefore varied in a systematic manner. The accelerating voltage of electrons impinging on  $\text{Nd}^{3+}:\delta\text{-Al}_2\text{O}_3$  nanopowders was adjusted together with the current so as to maintain constant excitation power. This alters the average depth at which light generation occurs while in principle maintaining a constant excitation rate of rare earth impurities. Light output in the spectral region of laser emission was then monitored closely to observe the behavior of the stimulated emission lines ( $<25,000$   $\text{cm}^{-1}$ ) and quenched transitions ( $>25,000$   $\text{cm}^{-1}$ ) described in Ref. 37.

Emission spectra obtained at constant excitation rate revealed a rapid rise in the Nd laser lines between 24,250  $\text{cm}^{-1}$  and 25,000  $\text{cm}^{-1}$  and an equally rapid decline of quenched transitions for voltages above 3 kV. This behavior is the same as that accompanying Nd random laser action (Fig. 4). The output intensity on the stimulated emission lines increased systematically with increasing voltage at constant excitation rate, as expected if optical confinement improves at larger distances from the surface (Fig. 5). Monte Carlo simulations (Fig. 6) revealed,

however, that the naïve experimental procedure of maintaining a constant voltage–current product did not succeed in maintaining a constant rate of excitation of rare-earth emitters. Between 2 and 10 kV, the distribution of electron penetration depth broadens by a factor of 10 [Fig. 6(a)] for alumina powder of 50% solid density as the penetration depth itself increases from 50 to 950 nm [Fig. 6(b)]. Since this lowers the active electron density in all three dimensions, the average rate of excitation by electrons is lower at 10 kV than at 2 kV by a large factor ( $\sim 10^3$ ), even though the voltage–current product is constant. Hence we observe an increase in laser output and slope efficiency, despite a decrease in the excitation rate, as the gain volume moves deeper into the powder.

## 5. STATIONARY LIGHT

By itself, the observation of cw laser action in a strongly scattering random medium does not indicate that light is generated in a nonpropagating or stationary state. However, the complete absence of modal and directional selectivity in the output, the apparent lack of coherence, and the short transport mean free path ( $l^* = \lambda/2$ ) do indicate a lasing process confined to an effective cavity with dimensions of a wavelength or less. While this conclusion currently relies to a significant degree on the surprisingly short  $l^*$  measured by coherent backscattering, independent measurement of the coherence length ( $l_{\text{coh}} < \lambda$ ) in laser speckle transmitted through a free-standing sample as reported here corroborates dephasing within subwavelength regions of the medium. Optical dephasing and directional scrambling over such small intervals shows that the light is overdamped or critically damped in the absence of significant absorption.

The inference is that electron pumping and dependent scattering mediate laser action in our samples by generating stationary light that experiences gain. The improvement of laser output at constant pumping power furnishes particularly direct and compelling evidence—with or without the Monte Carlo corrections for excitation rates at different depths—that light experiences dramatically improved confinement as the gain region is displaced from the surface into the bulk of the powder. If the surface provided reflective feedback, the opposite result would be expected. Our calculations and experiments support the idea that high-Q enhancement regions are responsible for stimulated emission and cw lasing deep within our powders, and that these regions extend approximately a wavelength in all three dimensions. By imputation, other regions of these dense samples must support tunneling, hopping conduction, or diffusion of electromagnetic waves over much longer distance scales to account for the long-range transmission properties of these intriguing materials.

In closing we remark that electron excitation has a potentially important advantage over photon generation of laser light within our samples. Both in photonic bandgap materials and random media, any high-Q cavities that may be present prevent the easy escape of light while at the same time making it difficult for pump-light at adjacent wavelengths to enter. Electrons, on the other hand, are not restricted from penetrating cavities or

pseudogap regions in photonic bandgap or random media. Optical fields can therefore be created inside any region within the penetration depth of incident electrons, regardless whether they are high-Q or low-Q, wavelength selective or not. Once the rare earth impurities are excited, we believe that the regions with highest field enhancement in our samples localize light and cause gain with feedback by virtue of interference effects from correlations in the disposition of particles of shorter range than those encountered in the diffusive propagation regime.<sup>43</sup> In previous work, we showed experimentally that with increased gain, cw laser action in ultrafine random media exhibits an apparent crossover from oscillator to amplifier behavior.<sup>29</sup> Low-voltage operation therefore seems to favor stationary laser light generation, whereas high-voltage operation encourages propagation with coherent amplification over macroscopic distances.

## 6. CONCLUSION

In conclusion we believe the evidence in this paper shows that it is possible in active, low-loss dielectrics with particle densities  $\gg 1/\lambda^3$  to generate regions of pointlike, stationary laser light. On the other hand, optical transport over macroscopic distances of the order of hundreds of micrometers has been observed in transmission through such samples. Extinction lengths of millimeters were measured in free-standing powder samples with transport lengths of only a few hundred nanometers. Hence, we are led to the realization that, at least for low-volume-fraction, random media, the distribution of particles and fields is very heterogeneous, and that the heterogeneity strongly influences electromagnetic propagation. Dense configurations of particles seem able to localize light in some regions, while sparse configurations permit propagation in others, which suggests that extended and localized states coexist in 3D samples in this regime. While many interesting fundamental questions remain regarding characteristics of the strong scattering regime, some practical aspects of these results can already be anticipated. Nanopowder light sources operating by stimulated emission may lead to improved phosphors for conventional fluorescent lighting and flat panel displays, and to completely new, electrically pumped laser sources operating at wavelengths throughout the ultraviolet, visible, and infrared spectral regions.

## ACKNOWLEDGMENTS

The authors acknowledge partial research support from the U.S. Air Force Office of Research under grant F49620-03-1-0389 and the National Science Foundation under grant DMR-9975542, and useful discussions with A. Genack and D. Wiersma.

Corresponding author S. C. Rand may be reached by e-mail to scr@eecs.umich.edu.

## REFERENCES

1. L. V. Hau, S. E. Harris, Z. Dutton, and C. H. Behroozi, "Light speed reduction to 17 meters per second in an ultracold atomic gas," *Nature* **397**, 594–598 (1999).
2. C. Liu, Z. Dutton, C. H. Behroozi, and L. V. Hau, "Observa-



- tion of coherent optical information storage in an atomic medium using halted light pulses," *Nature* **409**, 490–493 (2001).
3. A. V. Turukhin, V. S. Sudarshanam, M. S. Shahriar, J. A. Musser, B. S. Ham, and P. R. Hemmer, "Observation of ultraslow and stored light pulses in a solid," *Phys. Rev. Lett.* **88**, 023602 (2002).
  4. A. S. Zibrov, A. B. Matsko, O. Kocharovskaya, Y. V. Rostovtsev, G. R. Welch, and M. O. Scully, "Transporting and time reversing light via atomic coherence," *Phys. Rev. Lett.* **88**, 103601 (2002).
  5. A. Andre and M. D. Lukin, "Manipulating light pulses via dynamically-controlled photonic bandgap," *Phys. Rev. Lett.* **89**, 143602 (2002).
  6. M. S. Bigelow, N. N. Lepeshkin, and R. W. Boyd, "Observation of ultraslow light propagation in a ruby crystal at room temperature," *Phys. Rev. Lett.* **90**, 113903 (2003).
  7. J. D. Jackson, *Classical Electrodynamics*, 2nd ed. (Wiley, New York, 1975).
  8. J. D. Joannopoulos, *Photonic Crystals—Controlling the Flow of Light* (Princeton University, Princeton, N.J., 1995).
  9. See for example P. Sheng, *Introduction to Wave Scattering, Localization, and Mesoscopic Phenomena* (Academic, London, 1995).
  10. P. W. Anderson, "Absence of diffusion in certain lattices," *Phys. Rev.* **109**, 1492–1505 (1958).
  11. S. John, "Electromagnetic absorption in a disordered medium near a photon mobility edge," *Phys. Rev. Lett.* **53**, 2169–2172 (1984).
  12. P. W. Anderson, "The question of classical localization: a theory of white paint?" *Philos. Mag. B* **52**, 505–509 (1985).
  13. A. F. Ioffe and A. R. Regel, "Non-crystalline, amorphous and liquid electronic semiconductors," *Prog. Semicond.* **4**, 237–291 (1960).
  14. D. S. Wiersma, P. Bartolini, A. Lagendijk, and R. Righini, "Localization of light in a disordered medium," *Nature* **390**, 671–673 (1997).
  15. D. S. Wiersma, M. P. van Albada, B. A. van Tiggelen, and A. Lagendijk, "Experimental evidence for recurrent multiple scattering events in disordered media," *Phys. Rev. Lett.* **74**, 4193–4196 (1995).
  16. A. Z. Genack and N. Garcia, "Observation of photon localization in a three-dimensional disordered system," *Phys. Rev. Lett.* **66**, 2064–2067 (1991).
  17. A. A. Chabanov and A. Z. Genack, "Photon localization in resonant media," *Phys. Rev. Lett.* **87**, 153901 (2001).
  18. K.-J. Boller, A. Imamoglu, and S. E. Harris, "Observation of electromagnetically induced transparency," *Phys. Rev. Lett.* **66**, 2593–2596 (1991).
  19. M. Born and E. Wolf, *Principles of Optics*, 7th ed. (Cambridge University, Cambridge, U.K., 1999), p. 723.
  20. G. S. Agarwal and S. D. Gupta, "Reciprocity relations for reflected amplitudes," *Opt. Lett.* **27**, 1205–1207 (2002).
  21. See for example A. Siegman, *Lasers* (University Science, Sausalito, Calif., 1986).
  22. See for example K. Kamiuto, "Near-field scattering by a small spherical particle embedded in a nonabsorbing medium," *J. Opt. Soc. Am. B* **1**, 840–844 (1984).
  23. L. M. Zurk, L. Tsang, K. H. Ding, and D. P. Winnebrenner, "Monte Carlo simulations of the extinction rate of densely packed spheres with clustered and nonclustered geometries," *J. Opt. Soc. Am. A* **12**, 1772–1778 (1995).
  24. P. Gadenne, X. Quelin, S. Ducourtieux, S. Gresillon, L. Aigouy, J. C. Rivoal, V. Shalaev, and A. Sarychev, "Direct observation of locally enhanced electromagnetic field," *Physica B* **279**, 52–55 (2000).
  25. S. M. Redmond, "Luminescent instabilities and nonradiative processes in rare earth systems," Ph.D. dissertation (University of Michigan, Ann Arbor, Michigan, 2003).
  26. V. V. Klimov and V. S. Letokhov, "Enhancement and inhibition of spontaneous emission rates in nanobubbles," *Chem. Phys. Lett.* **301**, 441–448 (1999).
  27. N. Garcia, A. Z. Genack, and A. A. Lisyansky, "Measurement of the transport mean free path of diffusing photons," *Phys. Rev. B* **46**, 14475–14479 (1992).
  28. A. Z. Genack, "Optical transmission in disordered media," *Phys. Rev. Lett.* **58**, 2043–2046 (1987).
  29. G. R. Williams, S. B. Bayram, S. C. Rand, T. Hinklin, and R. M. Laine, "Laser action in strongly scattering rare-earth-metal-doped dielectric nanophosphors," *Phys. Rev. A* **65**, 013807 (2000).
  30. X. Jiang and C. M. Soukoulis, "Transmission and reflection studies of periodic and random systems with gain," *Phys. Rev. B* **59**, 6159–6166 (1999).
  31. L. Laversenne, Y. Guyot, C. Goutaudier, M. Th. Cohen-Adad, and G. Boulon, "Optimization of spectroscopic properties of Yb<sup>3+</sup>-doped refractory sesquioxides: cubic Y<sub>2</sub>O<sub>3</sub>, Lu<sub>2</sub>O<sub>3</sub> and monoclinic Gd<sub>2</sub>O<sub>3</sub>," *Opt. Mat.* **16**, 475–483 (2001).
  32. P. Sebbah, B. Hu, A. Z. Genack, R. Pnini, and B. Shapiro, "Spatial-field correlation: the building block of mesoscopic fluctuations," *Phys. Rev. Lett.* **88**, 123901 (2002).
  33. V. Emiliani, F. Intonti, M. Cazayous, D. S. Wiersma, M. Colocci, F. Aliev, and A. D. Lagendijk, "Near-field, short range correlation in optical waves transmitted through random media," *Phys. Rev. Lett.* **90**, 250801 (2003).
  34. P. A. Lee and A. D. Stone, "Universal conductance fluctuations in metals," *Phys. Rev. Lett.* **55**, 1622–1625 (1985).
  35. J. W. Goodman, *Statistical Optics* (Wiley, New York, 1985), p. 206.
  36. V. M. Markushev, V. F. Zolin, and C. M. Briskina, "Luminescence and stimulated emission of neodymium in sodium lanthanum molybdate powders," *Sov. J. Quantum Electron.* **16**, 281–283 (1986).
  37. N. M. Lawandy, R. M. Balachandran, A. S. L. Gomes, and E. Sauvain, "Laser action in strongly scattering media," *Nature* **368**, 436–438 (1994).
  38. S. V. Frolov, Z. V. Vardeny, K. Yoshino, A. Zakhidov, and R. H. Baughman, "Stimulated emission in high-gain organic media," *Phys. Rev. B* **59**, R5284–R5287 (1999).
  39. H. Cao, Y. G. Zhao, S. T. Ho, E. W. Seelig, Q. H. Wang, and R. P. H. Chang, "Random laser action in semiconductor powder," *Phys. Rev. Lett.* **82**, 2278–2281 (1999).
  40. R. K. Thareja and A. Mitra, "Random laser action in ZnO," *Appl. Phys. B* **71**, 181–184 (2000).
  41. B. Li, G. R. Williams, S. C. Rand, T. Hinklin, and R. M. Laine, "Continuous-wave ultraviolet laser action in strongly scattering Nd-doped alumina," *Opt. Lett.* **27**, 394–396 (2002).
  42. H. F. Arnoldus and J. T. Foley, "Spatial separation of the traveling and evanescent parts of dipole radiation," *Opt. Lett.* **28**, 1299–1301 (2003).
  43. C. Vanneste and P. Sebbah, "Selective excitation of localized modes in active random media," *Phys. Rev. Lett.* **87**, 183903 (2001).